Exact determination of electrical properties of wurtzite $Al_{1-x}In_xN$/(AlN)/GaN heterostructures ($0.07 \leq x \leq 0.21$) by means of a detailed charge balance equation

MARCUS GONSCHOREK, JEAN-FRANCOIS CARLIN, ERIC FELTIN, MARCEL PY AND NICOLAS GRANDJEAN

This paper discusses the determination of key electrical parameters of AlInN/(AlN)/GaN heterostructures from capacitance–voltage (CV) measurements. These heterostructures gained recently importance since they allow for high electron mobility transistor (HEMT) devices with several remarkable records: densities of the 2D electron gas (2DEG) of 2.6×10^{13} cm^{-2} for lattice-matched (LM) heterostructures and barrier thickness of 14 nm, beyond 2 A/mm saturation currents, above 100 GHz operation for heterostructures grown on Si (111) with gate length of 0.1 µm. Despite these striking experimental results, a consistent determination of the most important electrical parameters, namely polarization sheet charge density, surface potential, and dielectric constant of the alloy are still missing. By setting up the correct charge balance equation, these parameters can unambiguously be determined. For instance, in the case of nearly LM $Al_{0.85}In_{0.15}N$ these parameters amount to $\sigma_{Al_{0.85}In_{0.15}N/GaN} \sim 3.7 \times 10^{17}$ m^{-2}, $e\Phi_S \sim 3$ eV and $\varepsilon_{Al_{0.85}In_{0.15}N} \sim 11.2$, for the charge density, the surface barrier potential, and the dielectric constant, respectively.

Keywords: AlInN, High electron mobility transistor, Polarization charge, Capacitance–voltage, 2D electron gas

I. INTRODUCTION

A few years ago there was only scarce data on the AlInN alloy properties. Actually, the scientific work on this material system was intensified only since 2005. At that time, the well established material system for high power devices was AlGaN/GaN. These heterostructures exhibit typical 2D electron gas (2DEG) density confined at the heterointerface of the order of $\sim 1.0 \times 10^{13}$ cm^{-2}. Especially, high electron mobility transistors (HEMTs) operating at GHz frequencies processed from these heterostructures already reached market maturity and are nowadays successfully commercialized with a special interest in communication technologies such as "worldwide interoperability for microwave access".

However, it was found that lattice-matched (LM) AlInN/GaN heterostructures exhibit more than twice the amount of electrons confined at the heterointerface, i.e. in the order of 2.6×10^{13} cm^{-2} and hence there is a serious interest for the next generation of high power electronics. Unfortunately, these electrons forming the so-called 2DEG may suffer from poor in-plane transport properties due to alloy disorder scattering. Therefore, we used an approach already explored within the AlGaN/GaN system, namely the insertion of an AlN interlayer. This helps to keep the electrons better confined in the GaN channel and prevents 2DEG electrons from alloy

scattering within the AlInN barrier. The variation of the interlayer thickness thereby results in a "high mobility window" with a maximum of 1200 cm²/V s at an interlayer thickness of ~ 1 nm at room temperature (RT) [1]. HEMTs processed from these heterostructures exhibit saturation current densities up to 2 A/mm [2] and operate at frequencies up to 100 GHz for heterostructures grown on Si(111) substrate [3]. Such devices typically exhibit maximum power densities up to 10 W/mm at 10 GHz [4].

Details on the growth of these films can be found in refs. [5, 6]. However, the growth of high-quality AlInN films is a difficult task due to the large difference between InN and AlN covalent bonds, which might lead to phase separation and strong composition inhomogeneities. In this framework, we discuss here only epilayers that exhibit a coherent growth on GaN templates, which was verified with reciprocal space maps recorded with X-ray diffraction [7] in the composition regime $0.07 \leq x \leq 0.21$.

Since a thorough description of electrical properties of such AlInN/AlN/GaN heterostructures is still lacking in the literature it is the scope of this article.

II. BIAXIALLY STRAINED $Al_{1-x}In_xN$ ON GaN

A) Critical thickness

The generation of misfit dislocations (MDs) is a well-known phenomenon in heteroepitaxy, in which a thin film is grown on a substrate with a significantly different lattice parameter.

Institute of Condensed Matter Physics (ICMP), Ecole Polytechnique Fédérale de Lausanne (EPFL), CH-1015 Lausanne, Switzerland.
Corresponding author:
M. Gonschorek
Email: marcus.gonschorek@epfl.ch

Below a certain film thickness, called the critical thickness t_{cr}, a heteroepitaxial film may be grown pseudomorphically on a substrate, whereas a relaxation of misfit strain via plastic deformation occurs for thicker films $t > t_{cr}$. In this sense, the most common mechanism of plastic relaxation is through the formation of MDs.

Several theoretical models for calculating the critical thickness in isotropic materials have been published over the years [8–10]. Although they account reasonably well for the strain relaxation processes occurring in cubic systems such as SiGe/Si and InGaAs/GaAs, there has been only one report attempting to estimate the effect of hexagonal symmetry on the t_{cr} values [11]. Nevertheless, the model of Fischer et al. [8] provides a simple estimate for the critical thickness, namely $t_{cr} \sim b_e/2\varepsilon_{\|}$, with $b_e = 0.31825$ nm the length of the Burgers vector and the layer in-plane biaxial strain component $\varepsilon_{\|} = (a - a_o)/a_o$, with the strained lattice parameter a and its relaxed value a_o. Figure 1 shows t_{cr} expected for the onset of plastic relaxation via the formation of MDs for the $Al_{1-x}In_xN$ alloy grown on GaN with $a = 0.31825$ nm. The lattice matched condition is met at $x = 0.175$, where epilayers could potentially be grown infinitely thick. Experimentally, layer thicknesses of ~ 500 nm were achieved. In practice, t_{cr} drops rapidly below 100 nm within a $\pm 1\%$ range beside the LM condition. In the limits of the binary compounds, i.e. AlN and InN grown on c-plane GaN, the estimate yields $t_{cr} \sim 6.5$ nm for AlN/GaN, in very good agreement with experimentally results [12]. For InN/GaN, the experimental t_{cr} is found to be ~ 1 monolayer (ML), i.e. t_{cr} is slightly overestimated in Fig. 1. [13]. As indicated by the horizontal gray bar, the t_{cr} is > 15 nm in the composition regime $0.07 \le x \le 0.21$.

B) Spontaneous and piezoelectric polarizations

Understanding the polarization is crucial for accurately interpreting the optical and electrical properties in nitride
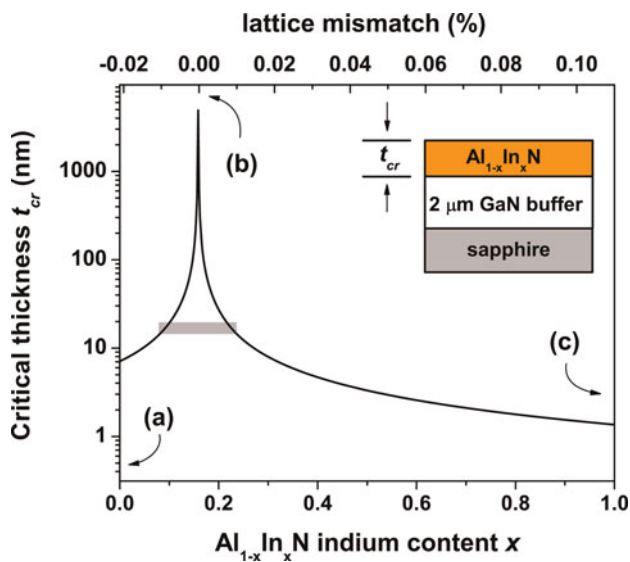

Fig. 1. Critical thickness t_{cr} expected for the onset of plastic relaxation via the formation of MDs for the $Al_{1-x}In_xN$ alloy grown on GaN with $a = 0.3182$ nm. The lattice matched condition is met at $x = 0.175$, where epilayers could potentially be grown infinitely thick. In practice, t_{cr} drops rapidly below 100 nm within a $\pm 1\%$ range from the LM condition.

heterostructures. The total polarization can be defined as the sum of the spontaneous polarization $P_{sp}(x)$ and the piezoelectric polarization $P_{pz}(x)$. The spontaneous polarization is an intrinsic property. In general, $P_{pz}(x)$ is described by a tensor but can be simplified for biaxially strained epilayers with growth in the [0001] direction as $P_{pz}(x) = 2\varepsilon_{\|}(e_{31} - e_{33} C_{13}/C_{33})$ with the piezoelectric constants e_{31} and e_{33}, and the elastic constants C_{13} and C_{33}. An extensive discussion can be found in ref. [14].

The polarization is basically a volume effect but since vicinal dipole sheets in the z-direction cancel out each other the polarization manifests itself at interface as the difference of the total polarization of neighboring layers. Thin pseudomorphic AlN layers grown on GaN exhibit therefore a higher total polarization charge density due to the significant contribution of the piezoelectric polarization. In the case of LM AlInN, this contribution vanishes completely and only the spontaneous polarization is present. Figure 2 displays the total polarization $P_{sp}(x) + P_{pz}(x)$ for III-nitride epilayers pseudomorphically grown on GaN as a function of their composition. Material parameters are taken from ref. [14]. If the polarization charge density is positive, electrons are attracted forming a 2DEG, if there is a plane of negative charges a 2D hole gas (2DHG) should be formed. Typically, AlGaN/GaN HEMTs are grown with a barrier Al content of $\sim 30\%$ giving rise to a t_{cr} of ~ 30 nm while holding a polarization charge density of 1.3×10^{13} cm^{-2}. For higher Al content, barriers tend to relax via MDs. From Fig. 2(a) it is clearly visible that LM AlInN/GaN heterostructures provide a polarization charge density which is twice the amount of typical $Al_{0.3}Ga_{0.7}N$/GaN heterostructures, and additionally, they are strain free.

III. ELECTROSTATICS OF AlInN/AlN/GaN HETEROSTRUCTURES: A BALANCE EQUATION MODEL

In the following, we are aiming to extract important parameters such as surface potential, polarization charges, and dielectric constant from our heterostructures. The ground state energy of the triangular quantum well located at the heterointerface is given by the variational solution as [15]

$$E_o(n_s) \approx \left(\frac{9\pi\hbar\, e^2 n_{2d}}{8\varepsilon_o\varepsilon_b(x)\sqrt{8m^*}} \right)^{2/3}, \qquad (1)$$

where $\hbar$ is the reduced Planck's constant, e the electron charge, n_{2d} the 2DEG sheet density, ε_o the permittivity of the free space, $\varepsilon_b(x)$ the relative dielectric constant, and m^* the electron effective mass. Now the balance equation can be set up going from the left to the right in the band diagram Fig. 2(b) respecting the AlN interlayer. In the following, we are referring to the concrete material, namely AlInN for the barrier, AlN for the interlayer, and GaN for the bulk. Then the balance equation can be written as

$$e\Phi_s(x) - E_{C,AlInN} \times d_{AlInN} + \Delta E_{C,AlInN/AlN}$$
$$- E_{C,AlN} \times d_{AlN} - \Delta E_{C,AlN/GaN}(x) + E_o$$
$$+ (E_F - E_o) = 0. \qquad (2)$$

Note that in this case $E_{C,\,AlN} = e(\sigma_{AlN/GaN} - n_{2d})/(\varepsilon_o\varepsilon_{AlN})$ is the field across the AlN interlayer and $E_{C,AlInN} = e(\sigma_{AlInN/AlN}(x) +$
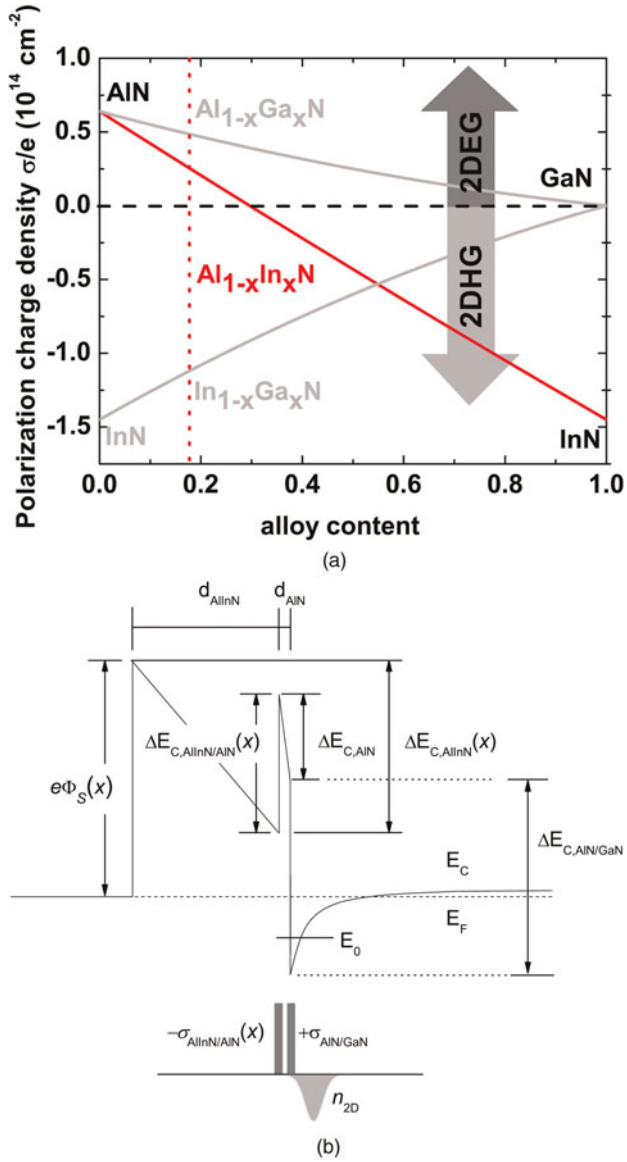
Fig. 2. (a) Polarization charge density bound at the heterointerface of the ABN/GaN heterostructure grown on Ga-face GaN [14]. Positive sign indicates the presence of a 2DEG whereas for negative polarization charges a 2DHG is expected. (b) Band diagram for the balance equation model of an AlInN/AlN/GaN heterostructure. Note the signs of the polarization across both heterointerfaces, which have crucial importance.

$\sigma_{AlN/GaN} - n_{2d})/(\varepsilon_o \varepsilon_{AlInN}(x))$ the field across the AlInN barrier. The latter is thus determined by the total polarization charge across the AlN interlayer.

The difference between the Fermi level E_F and the ground state energy E_o is given under the assumption that only one subband is filled as

$$E_F - E_o = \frac{\pi \hbar^2}{m^*} n_{2d}. \quad (3)$$

By setting $n_{2d} = 0$ in equation (2) allows determining the cases where the 2DEG is completely depleted, namely by a sufficiently thin barrier thickness t_{depl} via the pinned surface potential often also referred to as the "critical thickness"

(but this time to form the 2DEG):

$$t_{depl} = d_{AlN} + \left(e\Phi_s(x) + \Delta E_{C,AlInN/AlN} \right.$$
$$- \frac{e\sigma_{AlN/GaN}}{\varepsilon_o \varepsilon_{AlN}} \times d_{AlN} - \Delta E_{C,AlN/GaN}(x) \left. \right)$$
$$\times \frac{\varepsilon_o \varepsilon_{AlInN}(x)}{e\sigma_{AlInN/GaN}(x)} \quad (4)$$

and for the depletion voltage, i.e. the potential added to the built-in surface potential to completely deplete the 2DEG:

$$V_{depl} = \left(e\Phi_s(x) - \frac{e\sigma_{AlInN/GaN}(x)}{\varepsilon_o \varepsilon_{AlInN}(x)} \times d_{AlInN} \right.$$
$$+ \Delta E_{C,AlInN/AlN} - \frac{e\sigma_{AlN/GaN}}{\varepsilon_o \varepsilon_{AlN}} \times d_{AlN}$$
$$- \Delta E_{C,AlN/GaN}(x) \left. \right). \quad (5)$$

For a fixed interlayer thickness d_{AlN}, the slope of the depletion voltage for a given AlInN composition versus AlInN barrier thickness gives directly $\sigma_{AlInN/GaN}(x)/\varepsilon_{AlInN}(x)$. The offset at $d_{AlInN} = 0$ yields then

$$V_{d_{AlInN}=0} = (e\Phi_s(x) + \Delta E_{C,AlInN/AlN}$$
$$- e\sigma_{AlN/GaN}/\varepsilon_o \varepsilon_{AlN} \times d_{AlN}$$
$$- \Delta E_{C,AlN/GaN}(x)). \quad (6)$$

IV. 2DEG DENSITIES IN Al$_{1-x}$In$_x$N/ (AlN)/GaN HETEROSTRUCTURES

Usually, 2DEG densities are measured using capacitance voltage technique. However, this requires the fabrication of Schottky diodes, which is a time consuming task for nitride heterostructures contrary to arsenides. A way to overcome this problem is the use of electrochemical CV (ECV), where the Schottky contact is formed by an electrolyte/semiconductor interface. A suitable electrolyte for nitrides is H$_3$PO$_4$. For a given reverse bias point, the capacitance can then be probed by applying a small AC voltage. The advantage of ECV is now that the frequency of the AC voltage is a few kHz whereas in conventional CV the frequency is in the MHz regime. The former is clearly an advantage since large frequencies together with additional diode resistances can distort seriously measured CV curves [16, 17].

If a voltage is applied to the electrolyte the current flow induces an oxidation of the AlInN surface with a thickness of $\sim$1 nm. The capacitance for an oxide dielectric layer is given as

$$C_{ox} = \frac{\varepsilon \varepsilon_r}{d}. \quad (7)$$

Assuming that AlInN is transformed into Al$_2$O$_3$ with $\varepsilon \sim 12$ then C is $\sim$0.1 F/m^2. The total measured capacitance is then simply the capacitance of two capacitors in series according to

$$C_{tot} = \frac{CC_{ox}}{C + C_{ox}}, \quad (8)$$

where C is the true capacitance of the semiconductor heterostructure. In Fig. 3(a) the CV curves for $Al_{0.85}In_{0.15}N/AlN/GaN$ heterostructures are reported. Black lines indicate the *as measured* curves whereas gray curves indicate the corrected curves assuming 1 nm oxide layer. Thus the thin oxide layer leads therefore to a slight underestimation of the true 2DEG density, as can be seen from Fig. 3(a). On the other hand, the depletion voltage is not significantly shifted. Since the capacitance is defined as $C(V_{applied}) = edQ/dV$ the 2DEG densities n_{2d} can simply be obtained by integrating the corrected CV curves. By adding a term $V_{applied}$ to the balance equation (2) and fixing all other parameters except n_{2d}, solving for $n_{2d}(V_{applied})$ and taking the derivative of this expression one can also calculate the CV curves for a specific barrier thickness.

A) Extraction of electrostatic parameters for LM $Al_{0.83}In_{0.17}N/AlN(1\,nm)/GaN$ heterostructure

In Fig. 3(b) the depletion voltage versus AlInN barrier thickness is shown and gives, as can be expected from equation (5), a linear behavior. The slope $dV_{depl}/dd_{AlInN} = \sigma_{AlInN/GaN}(In = 0.15)/\varepsilon_0\varepsilon_{AlInN}(In = 0.15)$ is $\sim 6 \times 10^8$ V/m, or expressed in terms of $\sigma_{AlInN/GaN}(In = 0.15)/\varepsilon_{AlInN}(In = 0.15) \sim 0.332 \times 10^{17}$ m^{-2}. The offset at $d_{AlInN} = 0$ is ~ -1.05 V. However, as it can be seen from equation (6) this value is non-zero and determined by the other four non-vanishing expressions in equation (6). Figure 3(c) shows the integrated 2DEG densities from the uncorrected CV curves together with the Hall coefficients R_H at RT. Not considering the oxide films in CV analysis leads therefore to an underestimate of the correct 2DEG density. Note that R_H and CV results are in a very good agreement if the 1 nm oxide layer is considered.

We can now benefit from the information $\sigma_{AlInN/GaN}(In = 0.15)/\varepsilon_0\varepsilon_{AlInN}(In = 0.15) = 6 \times 10^8$ V/m and solve it for the unknown dielectric constant of the AlInN and plug the result back in equation (2). Now there are four unknown parameters namely the surface potential $e\Phi_S(x)$, polarization charge across the AlInN/AlN interface $\sigma_{AlInN/AlN}(x)$, the

dielectric constant of the alloy $\varepsilon_{AlInN}(x)$, and the critical thickness t_{cr}. For the other parameters it is assumed

$$d_{AlN} = 1.1\,\text{nm}, \quad \Delta E_{C,AlInN/AlN}(0.15) = 1.1\,\text{eV},$$
$$\sigma_{AlN/GaN} = 6.5 \times 10^{17}\,\text{m}^{-2},$$
$$e_{AlN} = 10.3, \quad \Delta E_{C,AlN/GaN} = 1.7\,\text{eV}. \tag{9}$$

Then the unknown parameters can be extracted by fitting data in Fig. 3(c) with equation (2) solved for $n_{2d}(d_{AlInN})$ yielding

$$e\Phi_s(0.15) = 2.9\,\text{eV},$$
$$\sigma_{AlInN/AlN}(0.15) = -2.8 \times 10^{17}\,\text{m}^{-2} \to \sigma_{AlInN/GaN}$$
$$\times (0.15) = 3.7 \times 10^{17}\,\text{m}^{-2},$$
$$e_{AlInN}(0.15) = 11.3,$$
$$t_{cr} = 2.3\,\text{nm}. \tag{10}$$

With the parameters we deduced the model well reproduces the experimental data in the whole thickness range. Note that equation (2) has an analytic solution which is unfortunately rather complex.

Note that these parameters are in excellent agreement with experimental results from the so-called electron holography method [18]. Indeed a voltage drop of ~ 2.5 eV across the LM 13 nm thick AlInN barrier was measured in good agreement with the electric field which can be calculated from the above parameters (10), which is discussed at the end of Section IV.C).

B) Variation of AlN interlayer thickness for LM $Al_{0.83}In_{0.17}N(13\,nm)/AlN/GaN$ heterostructure

Figure 4 displays the CV curves for an $Al_{0.85}In_{0.15}N/AlN/GaN$ heterostructure with a fixed AlInN thickness of ~ 12.5 nm and various AlN interlayer thicknesses from 0.6 to 2.1 nm. The inset shows the depletion voltage for different interlayer thicknesses. The behavior is not linear as in Fig. 3(b) and predicted by equation (5). The local slope for the thicker interlayers 1.7–
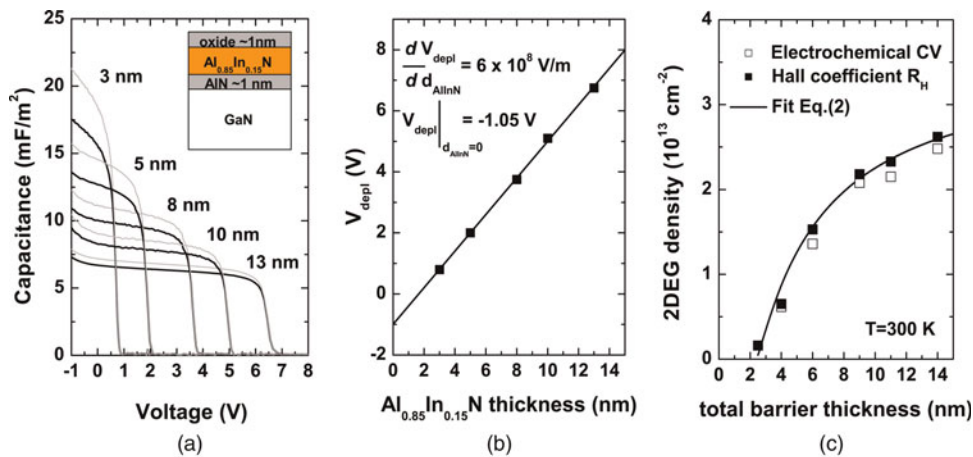

Fig. 3. (a) Electrochemical CV of an $Al_{0.85}In_{0.15}N/AlN/GaN$ heterostructure. The AlN interlayer thickness is 1.1 nm for all subfigures. During the measurement a ~ 1 nm thin layer at the AlInN surface is transformed into an oxide. Black curves are as measured and gray ones true CV considering the oxide. (b) Depletion voltages V_{depl} as a function of AlInN thickness. Slope and offset are indicated. (c) 2DEG density as a function of the total barrier thickness $d_{AlInN} + d_{AlN}$: obtained by RT Hall measurement (R_H) and integrated from the CV-curves in subfigure (a). The full line corresponds to equation (2) solved for $n_{2d}(d_{AlInN})$ together with the set of parameters (9) and (10).
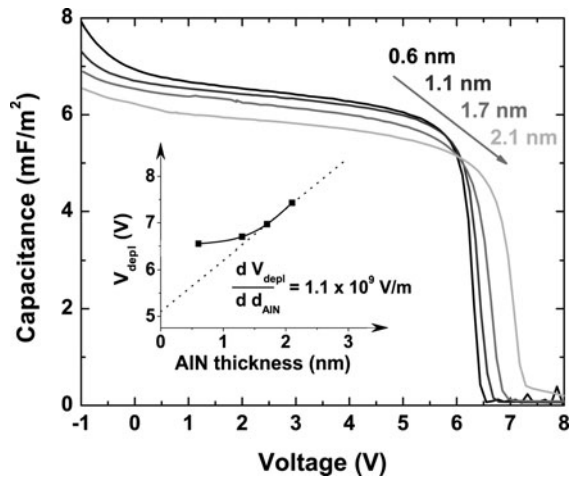
Fig. 4. *CV* curves for an $Al_{0.85}In_{0.15}N/AlN/GaN$ heterostructure with a fixed AlInN thickness of ~12.5 nm and various AlN interlayer thicknesses. Inset shows the depletion voltage for the respective interlayer thicknesses. The behavior is not linear as in Fig. 3(b). This is caused by thickness dependence of the surface potential and possibly due to a change in the static dielectric constant for these ultrathin layers. Local slope for thicker interlayers gives approximately the value expected for an AlN layer.

2.1 nm gives approximately the value expected for an AlN layer, namely $dV_{depl}/dd_{AlN} = e\sigma_{AlN/GaN}/\varepsilon_0\varepsilon_{AlN}$ is ~11 × 10^8 V/m, or expressed in terms of $\sigma_{AlN/GaN}/\varepsilon_{AlN} \sim 0.609 \times 10^{17}$ m^{-2}. In addition for a vanishing interlayer $d_{AlN} = 0$ one should make the transition from three-layer model equation (2) to the two-layer model by setting $d_{AlN} = 0$. A fit of depletion voltages for simple AlInN/GaN heterostructures (not shown here) yields again a slope $dV_{depl}/dd_{AlInN} = e\sigma_{AlInN/GaN}(In = 0.15)/\varepsilon_0\varepsilon_{AlInN}(In = 0.15)$ is ~6 × 10^8 V/m but with a slightly different offset of ~ −0.85 V. Assuming a conduction band offset at the single $Al_{0.85}In_{0.15}N/GaN$ hetero-junction of ~0.5 eV then the surface potential $e\Phi_s$ is according to $V_{depl}|_{dAlInN=0} = e\Phi_s - \Delta E_C(x)$ approximately 1.35 eV, i.e. is only half the value found in heterostructures with thicker interlayers. This implicit dependence of the surface potential and conduction band offset is not considered in equation (2).

C) Extraction of electrostatic parameters for non-LM $Al_{1-x}In_xN/AlN/GaN$ heterostructures $(0.07 \leq x \leq 0.21)$

Now we apply this procedure to obtain the electrostatic parameters for heterostructures with indium composition in the range $0.07 \leq x \leq 0.21$. In Fig. 5, the depletion voltages V_{depl} for 6 and 14 nm thick barriers as a function of $Al_{1-x}In_xN$ thickness for several compositions are shown. Black lines and gray lines indicate tensile and compressive regime, respectively. In Fig. 5(b) the 2DEG densities (integrated from *CV* curve) at RT for 6, 9, 14, and 33 nm thick $Al_{1-x}In_xN$ barriers on GaN epilayers (black squares) are depicted. Blue lines correspond to a fit using equation (2). A full line turning into a dashed line indicates that the critical thickness t_{cr}, beyond which pseudomorphic AlInN layers are expected to relax, is reached for the respective composition. Especially, the 14 nm barriers in the compressive regime exhibit similar 2DEG densities as the LM heterostructures causing similar depletion voltages. The electrostatic parameters are summarized in Table 1.

Since band offset in nitride heterostructures can only be hardly measured we make the following assumption for the AlInN/AlN interface: it has been demonstrated that the valence band offset of coherently strained InN(2 nm)/AlN (0001) is $\Delta E_{V,InN/AlN} \sim 3.1$ eV [19]. Furthermore, it has been shown that the valence band offset of $Al_{1-x}In_xN/GaN$ heterostructures scales linearly between the binary compositions [20]. Therefore, the band offset is estimated as $\Delta E_{C,AlInN/AlN} = E_{g,AlN} - E_{g,AlInN(x)} - x\Delta E_{V,InN/AlN}$, where the bandgap dependence of the AlInN alloy is taken from ref. [21]. Note that even in the case that the band offset of $Al_{0.0}In_{1.0}N/AlN(1 nm)/GaN$ behaves more as the band alignment of an InN/GaN heterostructure [22], i.e. negligible influence of the 1 nm AlN interlayer, the error in the low indium regime of the alloy on the band offset is minor since $\Delta E_{V,AlN/GaN} + \Delta E_{V,InN/GaN} \sim 1.5$ eV.

Figure 6(a) shows the 2DEG densities versus indium composition for 6 and 14 nm thick AlInN barriers and the extrapolated total bound sheet density $\sigma(x)/e$ obtained using equation (2). Additionally, the spontaneous $P_{sp}(x)$ and the piezoelectric $P_{pz}(x)$ polarizations and their sum is shown based on the calculations of the macroscopic polarization
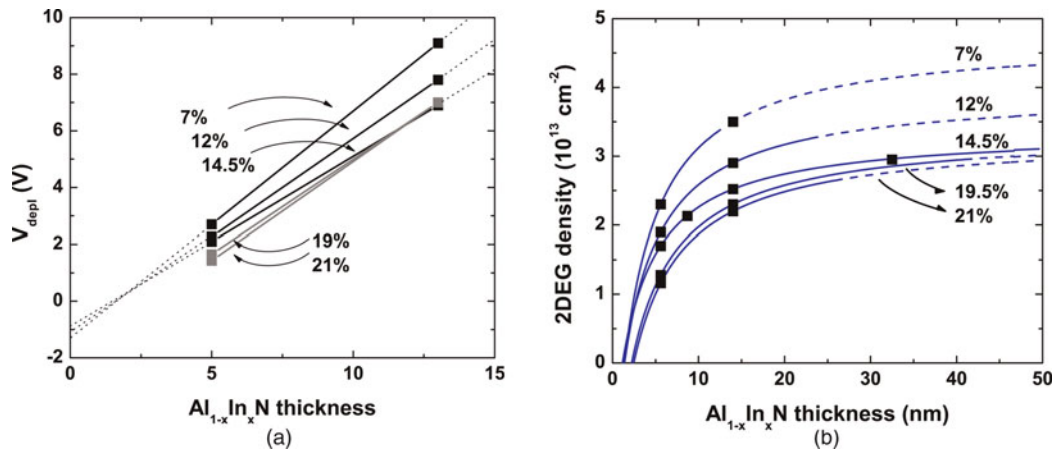

Fig. 5. (a) Depletion voltages V_{depl} for 6 and 14 nm thick barriers as a function of the $Al_{1-x}In_xN$ thickness for several compositions. Black and gray lines stand for the tensile and compressive regime, respectively. (b) 2DEG density (integrated from *CV* curve) at RT for 6, 9, 14, and 33 nm thick $Al_{1-x}In_xN$ barriers on GaN epilayers (black squares). Blue lines correspond to fits using equation (2). A full line turning into a dashed line indicates that the critical thickness t_{cr}, beyond which pseudomorphic AlInN layers are expected to relax, is reached for the respective composition.

Table 1. Critical thickness t_{cr} for plastic relaxation, 2DEG densities deduced from C–V measurements for 6 and 14 nm thick barriers, band offset at the AlInN/AlN interface, surface potential, and bound interface sheet density for five different compositions in the nearly LM regime between 7 and 21%.

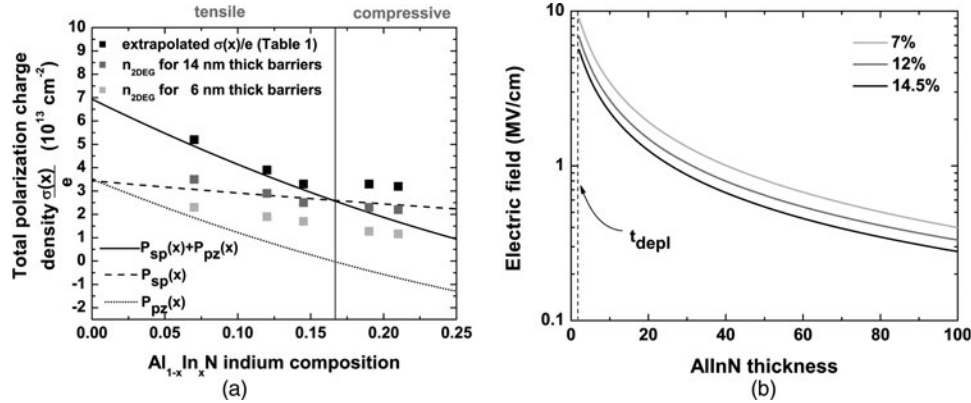| Indium content (%)	t_{cr} of $Al_{1-x}In_xN$ (nm)	2DEG density (10^{13} cm^{-2})		$\Delta E_{C,AlInN/AlN}$ (eV)	$e\Phi_b(x)$ (eV)	$\sigma(x)/e$ (10^{13} cm^{-2})	$\varepsilon_{AlInN}(x)$
		6 nm	14 nm				
7	13	2.0	4.0	0.5	4.4	5.4	10.8
12	25	1.6	2.9	1.0	3.4	4.2	10.9
14.5	52	1.5	2.6	1.2	3.0	3.7	11.2
19.5	45	1.3	2.3	1.5	2.6	3.3	~11.8
21	28	1.2	2.2	1.6	2.6	3.2	~11.8

Fig. 6. (a) Lines correspond to spontaneous (—) and piezoelectric (···) polarization charges and the sum of both (——) at RT for an AlInN random alloy. 2DEG densities for 6 nm thick (gray squares), 14 nm thick (dark gray squares) AlInN barriers, and the extrapolated total bound. (b) Electric field across the AlInN barrier for 7, 12, and 14.5% indium calculated from equation (2) using the parameters from Table 1.

for the AlInN random alloy as given by Bernardini and Fiorentini [23]. Indeed, these authors pointed out a strong nonlinear behavior for $P_{sp}(x)$ and $P_{pz}(x)$ depending on the atomic structure. Calculations were performed for a random alloy, i.e. a random distribution of group-III elements on the wurtzite cation sites, whereas anion sites are occupied by nitrogen leading to a P_{sp} bowing parameter $b_{random} \sim -0.065$ C/m^2 (black lines in Fig. 6(a)). For the tensile strain regime, extrapolated $\sigma(x)/e$ values agree fairly well with the trend expected for pseudomorphic layers, i.e. a contribution from $P_{pz}(x)$ is present. In the compressive regime (samples 19.5 and 21%), the $\sigma(x)/e$ values are much higher than expected for a pseudomorphic random alloy. Even the 2DEG densities for the 14 nm thick AlInN barriers exceed the polarization limit given by the black full line. This behavior might be caused by the following mechanism: it has been demonstrated that compressive AlInN relaxes favorably by building up a composition gradient by ending up with LM AlInN at the layer surface while keeping always the same in-plane lattice parameter [24]. Consequently, the compositional gradient in the AlInN causes a 3D "background" polarization with a positive sign throughout the barrier as demonstrated for graded AlGaN [15]. This "background" polarization can significantly increase the total polarization and consequently the amount of attracted electrons is increased.

From the last column in Table 1, namely the extracted dielectric constant of the AlInN alloy the behavior seems to be non-linear. This is consistent with the findings for bowing parameters of longitudinal optical phonon frequencies [25] and of refractive indices [26].

If the dependence of the 2DEG density on barrier thickness and polarization charge is known for a specific composition, the electric field across the AlInN barrier as a function of the barrier thickness can easily be calculated using the relation $E_{C,AlInN} = e(\sigma_{AlInN/AlN}(x) + \sigma_{AlN/GaN} - n_{2d}(d_{AlInN}))/(\varepsilon_o \varepsilon_{AlInN}(x))$, where $n_{2d}(d_{AlInN})$ is obtained from equation (2) and the parameters from Table 1 for the respective composition. The resulting field dependence is displayed in Fig. 6(b). Especially the optical properties depend sensitively on this electric field. Note that only for thicknesses below t_{depl}, i.e. for fully depleted 2DEG, the field is given exactly by $e\sigma_{AlInN/GaN}(x)/\varepsilon_o\varepsilon_{AlInN}(x)$.

V. CONCLUSIONS

A detailed charge balance equation was set up for $Al_{1-x}In_xN$/AlN/GaN heterostructures in order to extract important physical parameters around LM AlInN condition, i.e. $0.07 \leq x \leq 0.21$. These parameters can be extracted using the 2DEG density and the depletion voltage obtained from CV measurements for different barrier thicknesses. For nearly LM $Al_{0.85}In_{0.15}N$ these parameters amounts to $\sigma_{Al_{0.85}In_{0.15}N/GaN} \sim 3.7 \times 10^{17}$ m^{-2} for the polarization charge, $e\Phi_S \sim 3$ eV for the surface potential and $\varepsilon_{Al_{0.85}In_{0.15}N} \sim 11.2$ for the static dielectric constant. The voltage drop across the barrier for 13 nm thick $Al_{0.85}In_{0.15}N$ amounts to $\sim$2.5 eV which is in excellent agreement with the experimental value obtained from the electron holography method [18]. Especially the $Al_{1-x}In_xN$ static dielectric constant indicates a non-linear behavior between binaries with a bowing parameter b of $\sim$2–3 at $x = 0.15$.

ACKNOWLEDGEMENTS

REFERENCES

[1] Gonschorek, M. et al.: High electron mobility lattice-matched AlInN/GaN field-effect transistor heterostructures. Appl. Phys. Lett., **89** (2006), 062106.

[2] Medjdoub, F. et al.: Small-signal characteristics of AlInN/GaN HEMTs. Electron. Lett., **42** (2006), 779.

[3] Sun, H.F. et al.: 102-GHz AlInN/GaN HEMTs on silicon with 2.5-W/mm output power at 10 GHz. IEEE Electron Device Lett., **30** (2009), 796.

[4] Sarazin, N. et al.: AlInN/AlN/GaN HEMT technology on SiC with 10-W/mm and 50% PAE at 10 GHz. IEEE Electron Device Lett., **31** (2010), 11.

[5] Butte, R. et al.: Current status of AlInN layers lattice-matched to GaN for photonics and electronics. J. Phys. D: Appl. Phys., **40** (2007), 6328.

[6] Carlin, J.F. et al.: Crack-free fully epitaxial nitride microcavity using highly reflective AlInN/GaN Bragg mirrors. Appl. Phys. Lett., **86** (2005).

[7] Gonschorek, M. et al.: Two-dimensional electron gas density in Al1-xInxN/AlN/GaN heterostructures (0.03 ≤ x ≤ 0.23). J. Appl. Phys., **103** (2008), 093714.

[8] Fischer, A.; Kuhne, H.; Richter, H.: New approach in equilibrium-theory for strained-layer relaxation. Phys. Rev. Lett., **73** (1994), 2712.

[9] Matthews, J.W.; Blakeslee, A.E.: Defects in epitaxial multilayers. 1. Misfit dislocations. J. Cryst. Growth, **27** (1974), 118.

[10] People, R.; Bean, J.C.: Calculation of critical layer thickness versus lattice mismatch for Gexsi1-X/Si strained-layer heterostructures. Appl. Phys. Lett., **47** (1985), 322.

[11] Holec, D. et al.: Critical thickness calculations for InGaN/GaN. J. Cryst. Growth, **303** (2007), 314.

[12] Cao, Y.; Jena, D.: High-mobility window for two-dimensional electron gases at ultrathin AlN/GaN heterojunctions. Appl. Phys. Lett., **90** (2007), 182112.

[13] Yoshikawa, A. et al.: Fabrication and characterization of novel monolayer InN quantum wells in a GaN matrix. J. Vac. Sci. Technol. B, **26** (2008), 1551.

[14] Ambacher, O.; Cimalla, V.: Polarization Effects in Semiconductors: From Ab Initio Theory to Device Application, Springer, New York, 2007.

[15] Jena, D.: Polarization Effects in Semiconductors: From Ab Initio Theory to Device Application, Springer, New York, 2007.

[16] Blood, P.: Capacitance-voltage profiling and the characterisation of III–V semiconductors using electrolyte barriers. Semicond. Sci. Tech., **1** (1986), 7.

[17] Schroder, D.K.: Semiconductor Material and Device Characterization, Wiley, New York; Chichester, 1990, p. xv.

[18] Zhou, L. et al.: Polarization field mapping of Al0.85In0.15N/AlN/GaN heterostructure. Appl. Phys. Lett., **94** (2009), 121909.

[19] Wu, C.L.; Shen, C.H.; Gwo, S.: Valence band offset of wurtzite InN/AlN heterojunction determined by photoelectron spectroscopy. Appl. Phys. Lett., **88** (2006), 032105.

[20] King, P.D.C. et al.: Surface electronic properties of undoped InAlN alloys. Appl. Phys. Lett., **92** (2008), 172105.

[21] Iliopoulos, E. et al.: Energy bandgap bowing of InAlN alloys studied by spectroscopic ellipsometry. Appl. Phys. Lett., **92** (2008), 191907.

[22] King, P.D.C. et al.: InN/GaN valence band offset: high-resolution x-ray photoemission spectroscopy measurements. Phys. Rev. B, **78** (2008), 033308.

[23] Bernardini, F.; Fiorentini, V.: Nonlinear macroscopic polarization in III–V nitride alloys. Phys. Rev. B, **6408** (2001), 085207.

[24] Lorenz, K. et al.: Relaxation of compressively strained AlInN on GaN. J. Cryst. Growth, **310** (2008), 4058.

[25] Darakchieva, V. et al.: Lattice parameters, deviations from Vegard's rule, and E-2 phonons in InAlN. Appl. Phys. Lett., **93** (2008), 261908.

[26] Jiang, L.F.; Shen, W.Z.; Guo, Q.X.: Temperature dependence of the optical properties of AlInN. J. Appl. Phys., **106** (2009), 013515.

Marcus Gonschorek was born in Germany, in 1979. He received an M.S. degree in physics from the University of Leipzig, Germany, in 2005. His diploma work concerned arsenide-based quantum dot systems for non-volatile memory applications. He received his Ph.D. degree in physics from the Ecole polytechnique fédérale de Lausanne (EPFL), Switzerland, in 2009. The work concerned AlInN/AlN/GaN heterostructure and their application for high power electronic devices. His main research interests are fundamental properties of III–V semiconductor hetero- and quantum structures, carrier transport, and optoelectronic properties.

Jean-Francois Carlin was born in Nice, France, in 1962. He was graduated from the Ecole Centrale de Lyon in 1986 and made his doctoral research on the growth of GaInAsP compounds by chemical beam epitaxy at the Institute of Micro and Optoelectronics of the EPF-Lausanne, where he obtained the doctoral degree in 1993. He has been working on the growth and characterization of long wavelength vertical cavity lasers, microcavity light emitting diodes, and dual-wavelength coupled-cavity surface-emitting laser. He joined the field of III-nitride semiconductors in 2002, where he developed AlInN materials for optoelectronics and electronics. He is presently leading research effort on the growth of these wide bandgap nitride semiconductors in LASPE laboratory, at EPF-Lausanne.

Eric Feltin obtained his Ph.D. in physics from the University of Nice-Sophia Antipolis in 2003. His doctoral research at CNRS-CRHEA allowed new development in the growth of GaN on silicon substrates by MOVPE for the realization of light emitting diodes. He developed a new method for producing high-quality free-standing GaN substrates still used in the industry. He joined the Laboratory of Advanced Semiconductors for Photonics and Electronics at EPFL in 2004 where he worked on growth and technology of wide-bandgap semiconductors (GaN and its alloys) with particular emphasis on microcavities, VCSELs, and high electron mobility transistors. In 2009 he founded NOVAGAN, a company manufacturing III-nitride epitaxial wafers designed for UV-blue laser diodes and high frequency/power electronics. He is the author or coauthor of more than 80 publications in peer-reviewed international journals and holds one patent.

Marcel Py was born in Switzerland in 1950. He received the Ph.D. degree in physics at EPFL for an infrared and Raman study of the lattice vibrations in the MoO_3 layered compound. From 1980 to 1984, he was a post-doctoral fellow/research associate at the University of British Columbia, Vancouver, Canada, working on lithium intercalated layered compounds for high-energy storage. Since 1984, he is a scientific collaborator in the Institute of Quantum Electronics and Photonics at EPFL. He first worked on the MBE growth by solid sources of III-arsenide compounds and 2D electron gas heterostructures for HEMT applications. He then focused on the electrical characterization of such systems, by Hall effect for their transport properties, by deep level transient spectroscopy and low frequency noise (LFN) measurements.

Nicolas Grandjean was born in France and received his Ph.D. degree in physics from the University of Nice-Sophia Antipolis, in 1994. He was working during his Ph.D. thesis on III–V semiconductor based heterostructures. From 1994 to 2003, he was a member of the permanent staff at CNRS-France. His research activities were focused on the physical properties of nitride-based nanostructures, as well as on the realization of short-wavelength light emitters and UV detectors. In 2004, he has been appointed "Tenure-Track" Assistant Professor at Ecole Polytechnique Fédérale de Lausanne (EPFL)-Switzerland in the Institute of Quantum Photonics and Electronics. He was promoted full professor in 2009. He has been awarded the Sandoz Family Foundation grant for Academic Promotion. He is author or co-author of more than 300 publications in peer-reviewed international journals, five book chapters and holds four patents. His current research activities are centered on the growth, physics, and technology of wide-bandgap semiconductors (GaN and its alloys), and in particular on microcavities, quantum dots, intersubband transitions, and 2D electron gas heterostructures.